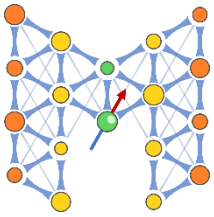

MANNGA Deliverable

D2.1 List of fabricated and characterised 1D and 2D transition metal CMRs on LPE YIG media, including their descriptions and measured KPIs

Version 1.0

Grant Agreement number	101070347
Action Acronym	MANNGA
Action Title	MAGNONIC ARTIFICIAL NEURAL NETWORKS AND GATE ARRAYS
Call	HORIZON-CL4-2021-DIGITAL-EMERGING-01
Version date of the Annex I against which the assessment will be made	31.5.2022
Start date of the project	1.9.2022
Due date of the deliverable	31.08.2023
Actual date of submission	31.08.2023
Lead BEN / AP for the deliverable	AALTO
Dissemination level of the deliverable	Public

Coordinator, PI
Sebastiaan van Dijken
AALTO KORKEAKOULUSÄÄTIÖ SR, Aalto University School of Science

Scientific coordinator
Volodymyr Kruglyak
THE UNIVERSITY OF EXETER

Co-funded by the European Union

MANNGA project is partly funded by the European Union. Views and opinions expressed are however those of the author(s) only and do not necessarily reflect those of the European Union or HADEA. Neither the European Union nor the granting authority can be held responsible for them.

Authors in alphabetical order		
Name	Beneficiary	e-mail
Sebastiaan van Dijken	Aalto University (AALTO)	sebastiaan.van.dijken@aalto.fi

Document reviewers		
Name	Beneficiary	e-mail
Volodymyr Kruglyak	University of Exeter (UNEXE)	V.V.Kruglyak@exeter.ac.uk

Executive summary

This deliverable report provides an overview of the fabricated and characterised 1D and 2D transition metal chiral magnonic resonators (CMRs) on liquid-phase epitaxy (LPE) YIG media. The resonator structures consist of a continuous YIG film with CoFeB micro- and nanostructures patterned on top. Different CoFeB structures were fabricated by e-beam lithography, including rectangles, disks, ellipses, and arrangements of multiple resonators. The structures were characterized by super-Nyquist sampling magneto-optic Kerr effect (SNS-MOKE) microscopy. Key parameters such as the modulation of the spin-wave amplitude and phase were measured as a function of magnetic bias field, spin-wave excitation frequency, and excitation power.

Contents

1. Metal CMR fabrication

Metal CMRs comprising a continuous YIG film and CoFeB micro- and nanostructures, separated by a thin insulating layer were fabricated by e-beam lithography at AALTO. To optimize the fabrication process, a 100 nm thick YIG film grown by pulsed laser deposition was used as the first sample. The CoFeB structures were patterned by e-beam lithography and lift off. The sample contained a large variety of CoFeB structures with different shapes and sizes. Shapes included rectangles, disks, and ellipses. Structures with multiple CMRs were also fabricated. A 1.5 µm wide Au microwave antenna was patterned 20 µm away from each CMR structure for spin-wave excitation. Examples of two fabricated structures are shown in Fig. 1. After the first sample, CMRs were patterned onto 100 nm LPE YIG, provided by INNOVENT. Two sample were fabricated using the same CoFeB nanostructure designs. The width of the microwave antennas on these two samples was reduced to 1.0 µm to broaden the spin-wave excitation range. The two samples with CoFeB CMRs were fabricated for complementary measurements at AALTO and MLU.

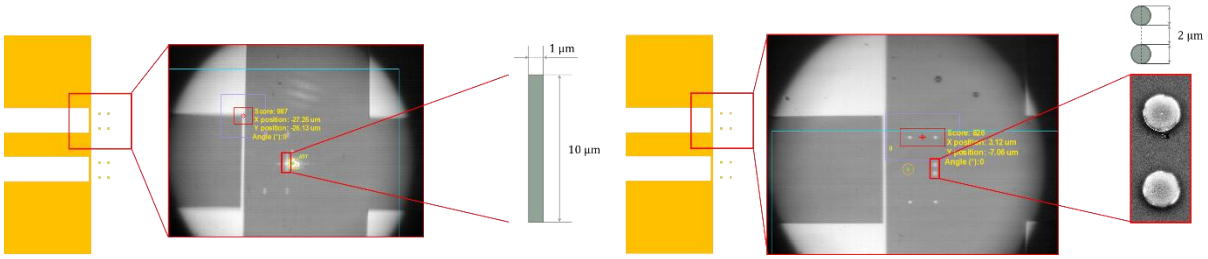

Fig. 1. Examples of fabricated metal CMRs. A CoFeB rectangle (left) and two CoFeB disks (right) on top of YIG. A microwave antenna is patterned left from the CMRs for spin-wave excitation. The interaction between spin waves and the CMRs is imaged by SNS-MOKE microscopy.

2. Metal CMR characterization

Various CoFeB CMRs were characterized by SNS-MOKE at AALTO. We mainly focused on CoFeB rectangles of different width and length to investigate the effect of length reduction (transition from 1D to 2D). From previous work we know that long CoFeB nanostripes on YIG films operate as magnonic Fabry-Pérot resonators. In such resonators, destructive interference between incoming spin waves and circulating spin waves within the CoFeB/YIG bilayer suppresses spin-wave transmission at discrete frequencies. The formation of transmission gaps for much shorter resonators is an open question. Moreover, additional effect such as diffraction from 2D CMR edges and the formation of caustic beams could occur. To answer these questions, and to assess the suitability of metal CMRs for integrated scattering networks later in MANNGA, we characterized the interaction of spin waves with rectangular CoFeB CMRs of different length and width. As key performance indicators we focused on the modulation of the spin-wave amplitude and phase. The dependence of these parameters on frequency, magnetic bias field (magnetization alignment in YIG and CoFeB), and spin-wave excitation power was gauged.

2.1 1D versus 2D CoFeB CMRs

Figure 2 shows frequency versus magnetic field data for 2.5 µm long and 10 µm long rectangular CoFeB CMRs. The data are recorded by SNS-MOKE just behind the CoFeB rectangles. Clear transmission gaps

are observed for the longer CMR structure. Shifts in the positions of the gaps are caused by independent switching of the magnetization in the YIG film and the CoFeB layers. In the measurement, the magnetic field is swept from negative to positive values. The magnetization in the two magnetic layers is therefore aligned parallel at negative field and larger positive field, but antiparallel between +1 mT and +6 mT. The frequency shift is explained by different spin-wave dispersions within the CoFeB/YIG bilayer for the parallel and antiparallel magnetization state, in agreement with micromagnetic simulations. Contrary to the 10 × 1 µm CMR, clear spin-wave transmission gaps are not measured behind the 2.5 × 1 µm CMR (Fig. 2, left panel). The experiments clearly demonstrate that the transition from 1D to 2D CMR structures results in weaker Fabry-Pérot-like behavior. Figure 3 shows SNS-MOKE microscopy images of spin-wave scattering on the same CoFeB CMRs. The measurements indicate a strong reduction of the spin-wave signal along triangularly shaped paths that originate at the CMR edges.

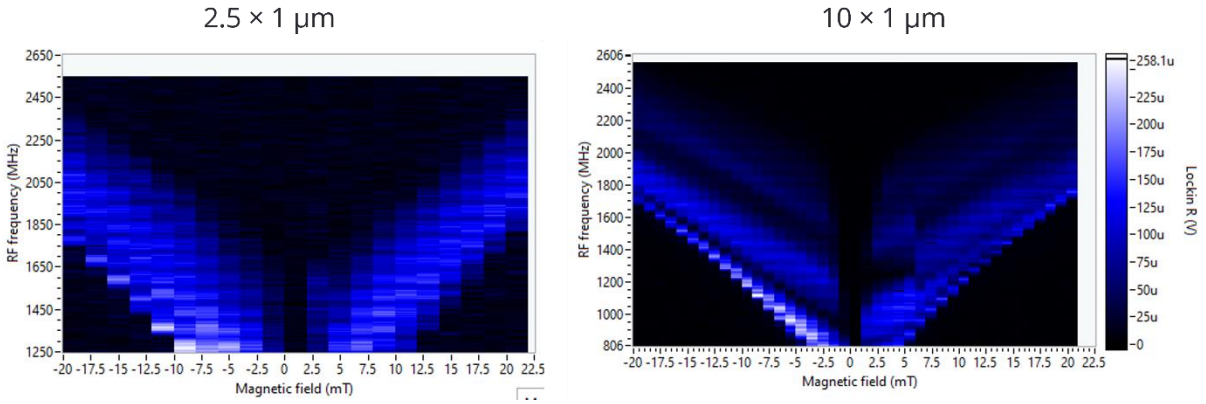

Fig. 2. Frequency versus magnetic field data for 2.5 µm long and 10 µm long rectangular CoFeB CMRs. The width of the CoFeB rectangles is 1 µm. The spectra are recorded by SNS-MOKE just behind the CMRs.

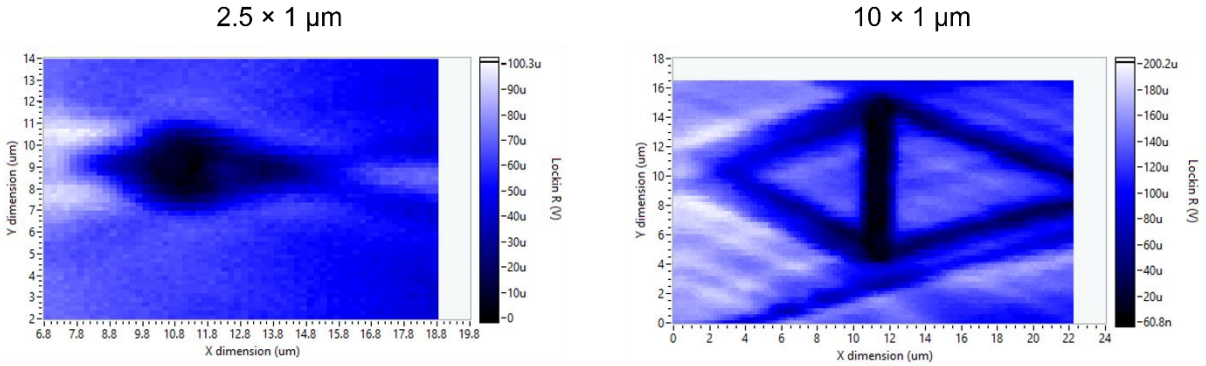

Fig. 3. SNS-MOKE microscopy images of spin-wave scattering on 2.5 µm long and 10 µm long rectangular CoFeB CMRs. The width of the CoFeB rectangles is 1 µm.

2.2 Modulation of the spin-wave phase

Besides the modulation of the spin-wave amplitude by CMRs, the modulation of the spin-wave phase is crucial for magnonic neural networks based on spin-wave scattering and wave interference. We measured the modulation of amplitude and phase as a function of frequency and magnetic bias field

on a 10 × 0.75 µm CMR exhibiting a clear transmission gap. Figure 4 shows spin-wave transmission spectra for parallel and antiparallel magnetization alignment. The spectra are recorded by SNS-MOKE microscopy at -4 mT. For both magnetization states we imaged the transmission of spin-waves across the CMR at different frequency, both inside and outside the transmission gap (see red arrows in Fig. 4). Figure 5 shows an overview of the measurement results. We plot the out-of-plane magnetization (m_z), the spin-wave amplitude, and the spin-wave phase. The spin-wave amplitude is reduced strongly behind the CMR at the gap frequency and along the triangular shaped paths that originate at the CMR edges (see discussion in previous section). The spin-wave phase is shifted behind the CMR by about π and the phase shift decreases further away from the CMR. Besides the data for parallel and antiparallel magnetization, we also recorded amplitude and phase data for two distinctive parallel configurations (+8 mT and -8mT). Because of the chirality of the resonator, the transmission of spin waves is different for the two parallel states. We are currently interpretating the CMR data using micromagnetic simulations.

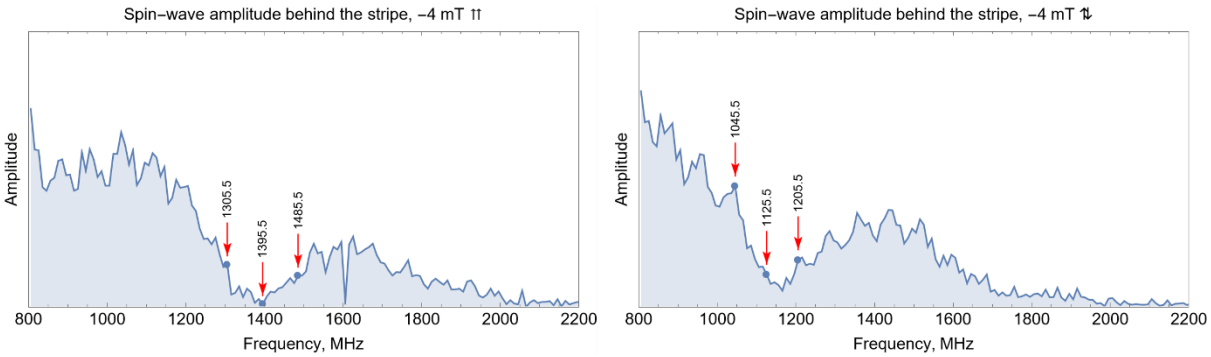

Fig. 4. Spin-wave transmission spectra of a 10 × 0.75 µm CMR measured for parallel (left) and antiparallel (right) magnetization in the CoFeB and YIG layers. The magnetic bias field is -4 mT in both measurements. The spectra are recorded by SNS-MOKE just behind the CMR.

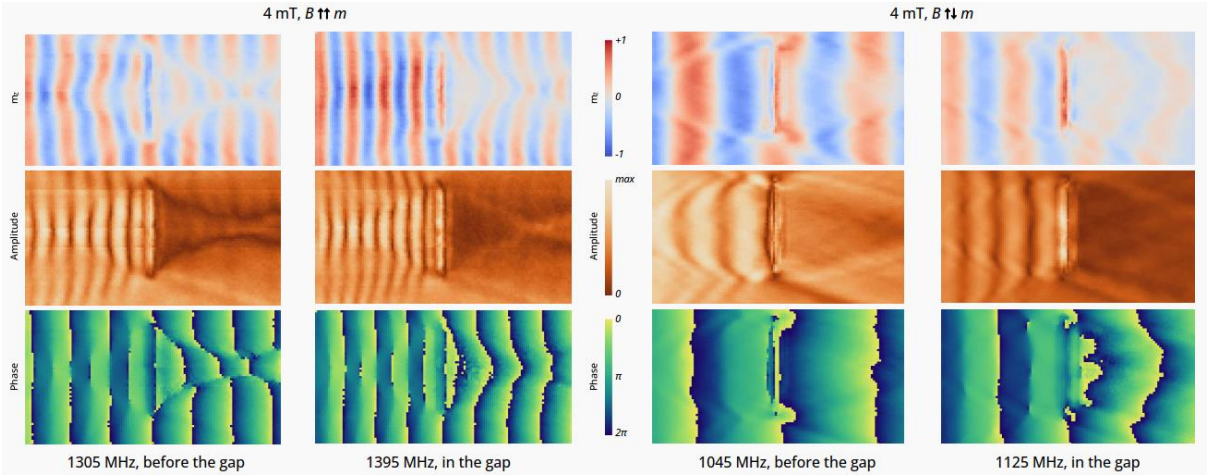

Fig. 5. SNS-MOKE microscopy images showing the interaction between propagating spin waves and a 10 × 0.75 µm CoFeB CMR. The panels show the out-of-plane magnetization (m_z), the spin-wave amplitude, and the spin-wave phase for parallel (left) and antiparallel magnetization alignment (right). The frequency is either just before or inside the spin-wave transmission gap (see also Fig. 4).

2.3 Dependence of CMR properties on spin-wave excitation power

Nonlinearity is an essential property of magnonic neural networks. We have measured the dependence of CMR properties on the spin-wave excitation power. Representative results are shown in Fig. 6 for a 10 × 1 µm CMR. More measurements on non-linearities will be conducted at AALTO and MLU.

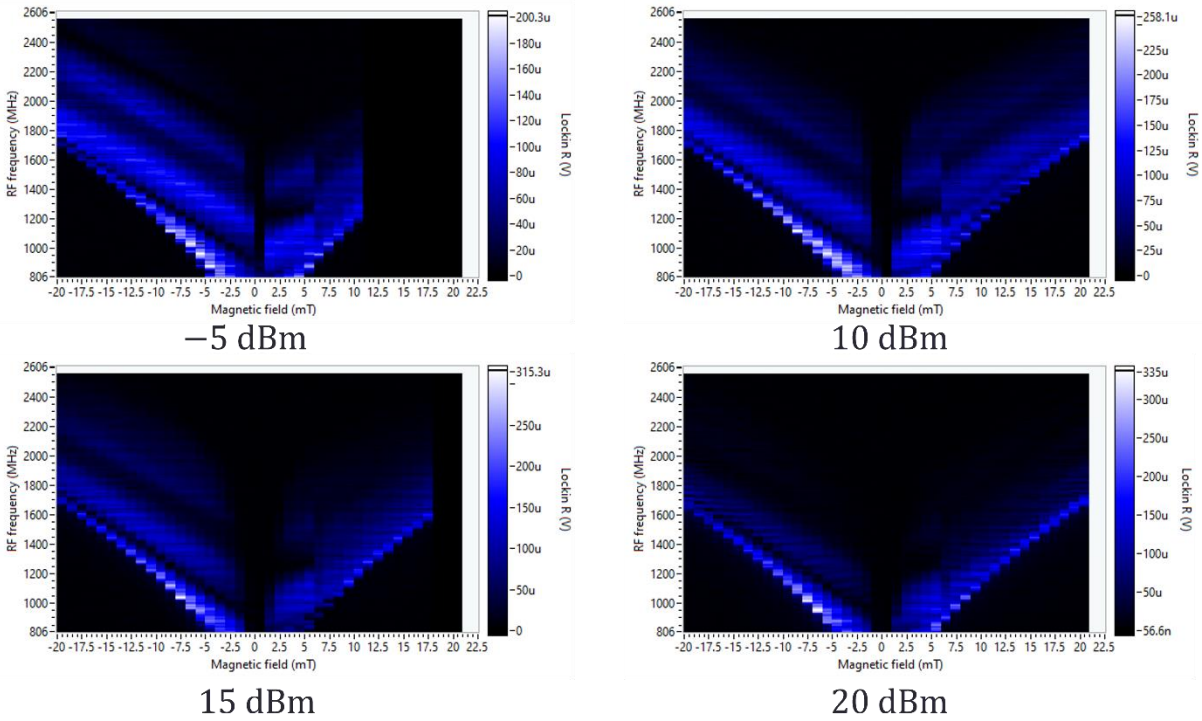

Fig. 6. Frequency versus magnetic field data for a 10 × 1 µm CoFeB CMR measured at different excitation power. The spectra are recorded by SNS-MOKE just behind the CMRs.